

# Development and preclinical assessment of nanoemulgel loaded with phytoconstituents for the management of rheumatoid arthritis

**Anita Chando**

Madison Ortho

**Vivek Basudkar**

Dr Bhanuben Nanavati College of Pharmacy Department of Pharmaceutics

**Sankalp Gharat**

Dr Bhanuben Nanavati College of Pharmacy Department of Pharmaceutics

**Munira momin** (✉ [munira\\_momin@yahoo.com](mailto:munira_momin@yahoo.com))

Dr Bhanuben Nanavati College of Pharmacy Department of Pharmaceutics <https://orcid.org/0000-0001-5908-2627>

**Tabassum Khan**

Dr Bhanuben Nanavati College of Pharmacy Department of Pharmaceutical Chemistry

---

## Research Article

**Keywords:** nanoemulgel, rheumatoid arthritis, ginger oleoresin, lipid guggul extract

**Posted Date:** May 9th, 2023

**DOI:** <https://doi.org/10.21203/rs.3.rs-2859476/v1>

**License:**  This work is licensed under a Creative Commons Attribution 4.0 International License.

[Read Full License](#)

---

# Abstract

In recent years, natural ingredients have gained importance for therapeutic treatment due to their minimal toxicity. However, the delivery of these phytoconstituents poses a challenge to provide better efficacy. Current research reports the development of nanoemulgel (NEG) loaded with ginger oleoresin (GOR) and lipid guggul extract (LGE) for the management of rheumatoid arthritis (RA). The nanoemulsion (NE) was developed using the spontaneous emulsification technique by the pseudo-ternary method. The optimized nanoemulsion exhibited globule size of  $16.08 \pm 2.55$ , PDI of  $0.187 \pm 0.06$  and Zeta Potential of  $-22.4 \pm 0.31$ . The cumulative release from *in-vitro* diffusion studies at pH 7.4 was about  $99.72 \pm 3.47\%$ ,  $57.98 \pm 2.11\%$  and  $86.42 \pm 5.13\%$  of 6-gingerol, E-guggulsterone and Z-guggulsterone respectively at the end of 24 hours. The *ex vivo* studies on porcine ear skin showed sustained release with  $92.8 \pm 3.21\%$  for 6-gingerol,  $55.61 \pm 0.91\%$  for E-guggulsterone, and  $84.2 \pm 4.22\%$  for Z-guggulsterone released at the end of 24 hours. The cell culture studies on RAW 264.7 cells indicated a robust inhibition of LPS-induced IL-6 and TNF- $\alpha$  production indicating its efficacy in the management of RA. The Preclinical studies on male Wistar rats suggests that the developed NEG exhibited a comparable decrease in paw edema inflammation as compared to the marketed diclofenac sodium gel. These encouraging results demonstrates the potential of the developed nanoemulgel containing combination of GOR and LGE for the management of RA.

## Introduction

Rheumatoid arthritis (RA) is a chronic immune-mediated disorder characterized by persistent inflammation, swelling and stiffness of joints due to synovial hyperplasia and pannus formation [1, 2]. According to WHO reports, generally RA develops between age of 20 and 40 being the most productive age of humans that often leads to pain, deformity and chronic disabling conditions and loss of quality life [3]. Young children below the age of 16yrs having RA are referred as juvenile rheumatoid arthritis (JRA) [4, 5]. Recent epidemiological study shows that the prevalence of RA is about 0.24% – 1% in developed countries and affects a greater number of women (2–3 times) than men. The RA may be diagnosed as early as three months from onset to two years when the disease is established [6]. Progression of RA is associated with difficulties in the day-to-day activities, leading to physical disability. A recent survey demonstrated that within 10 years of onset of RA, more than 50% patients in developed countries discontinued from a full time job [3].

Rheumatoid arthritis develops in patients due to various factors comprising of genetic and/or environment. Cytokine and T-cell signaling plays a critical role in the progression of RA [7]. The synovial inflammation and articular destruction associated with RA is characterized by elevated levels of pro-inflammatory cytokines such as IL-6, IL-1 $\beta$  and tumor necrosis factor (TNF- $\alpha$ ) along with prostaglandin E2 (PGE2) and nitric oxide (NO). It has been observed that the level of pro-inflammatory cytokines are more than compared to anti-inflammatory cytokines in patients with RA, this further accelerates the activity of other cytokines leading to destruction of bone and cartilage. IL-1 is one of the primary pro-inflammatory cytokines secreted by synovial macrophages, which plays significant role in progression of RA by exerting multiple biological effects such as synthesis of collagenase, PG, stimulation of fibroblasts,

and chemotaxis for B and T cells. TNF- $\alpha$  is another important cytokine, which is abundantly found in the rheumatoid joints as well as circulation and stimulates PGE<sub>2</sub> and collagenase, induces bone resorption, inhibits bone formation and production of matrix metalloproteinases (MMPs) [3, 8]. Recent developments in the technology of diagnostic have helped to detect and understand the underlying mechanism of RA however the exact pathology is still unknown [9].

Currently RA treatment modalities provide symptomatic relief that includes anti-inflammation medicines, steroids, analgesics, disease modifying anti-rheumatic drugs (DMARDs) and monoclonal antibodies (MAbs). Nonetheless, these drugs also have plenty of adverse effects, including digestive problems, renal toxicity, loss of protein, toxicity and immunosuppressive effects, all of which contribute to poor patient compliance [10, 11]. As a result, plant-based treatments are now being explored for the management of rheumatoid arthritis. Ginger oleoresin (GOR) contains shogaols and gingerols, which are found to inhibit cyclooxygenase 2 (COX-2), because of which it possesses anti-inflammatory property. 6-gingerol is also known to inhibit prostaglandin (PG) and leukotriene biosynthesis through suppression of 5-lipoxygenase (5-LOX) and PG synthetase. Further inhibition of synthesis of the pro-inflammatory cytokines such as IL-1 $\beta$ , IL-6, and TNF- $\alpha$  leads to the anti-inflammatory activity [12, 13]. Lipid guggul extract (LGE) is reported for anti-inflammatory activity by ameliorating the levels of pro-inflammatory mediators such as IL-6, TNF- $\alpha$ , IL-1 $\beta$ , NO, IL-12 and IFN- $\gamma$ . E and Z- guggulsterones decrease the levels of pro-inflammatory cytokines like IL-1 $\beta$ , IL-2, TNF- $\alpha$  and suppresses cyclooxygenase-2 (COX-2) mRNA levels, thereby demonstrates anti-inflammation and anti-arthritic activity [14, 15]. Both the drugs are lipophilic in nature, hence delivering in the form of nanoemulsion can increase their efficacy and suppress side effects in the management of RA.

Nanoemulsion (NE) is a biphasic colloidal dispersion of two immiscible liquids that are thermodynamically stable and thermodynamically unstable. NE has a lipidic interior and are a good choice for delivering and improving the bioavailability of lipophilic or hydrophobic drugs / extracts. In NE, Brownian motion dominates gravitational forces due to their smaller droplet size, thereby favoring a high kinetic stability towards flocculation, interface deformation, coalescence, etc. NE are preferred choice for drug delivery due to smaller-sized droplets, therefore provides greater surface area and greater absorption. In addition, they have high drug loading capacity, provides sustained or controlled release, and have higher drug penetration properties [16–19]. However, low viscosity of nanoemulsion leads to low retention rate at the site of application [20]. Hence, NE is incorporated into gel to overcome the drawbacks. In the present study, nanoemulsion was formulated using emulsification technique by the pseudo-ternary method containing GOR and LGE for the therapeutic treatment of RA. Further, nanoemulsion was incorporated into Carbopol gel to form nanoemulgel. The developed formulation was evaluated on various parameters including in-vitro diffusion studies, ex vivo permeation studies, HET CAM's studies, preclinical studies on CFA induced wistar rats RA model.

## Materials and methods

Ginger oleoresin (GOR) and Fenugreek oil was kindly gifted from Sunpure Extracts Pvt Ltd, Delhi, India. Lipid guggul extract (LGE) was received as a gift sample from Arjuna Naturals Pvt Ltd, Kerala, India. Castor oil and Capmul MCM was gifted from Jayant Agro-Organic Ltd, Mumbai, India and Abitec Corporation, USA respectively. Tween 80 and Kolliphor EL was given as a gift sample from Mohini Organics, Ltd, India and BASF, Mumbai, India respectively. Carbopol Ultrez 10 NF was provided as a gift sample from Lubrizol Advanced Materials India Pvt Ltd. Oleic acid, Transcutol P and Propylene glycol was purchased from Otto Chemie Pvt Ltd, Mumbai. India.

## **Formulation development**

### **Screening of oils, surfactants, and co-surfactants**

As GOR and LGE are liquids, selection of oil phase and surfactant phase were determined on the miscibility of these phytoconstituents in numerous oils, surfactants, and co-surfactants. Castor oil and Fenugreek oil were selected as functional excipients as they are known for anti-inflammatory activity [21, 22]. However, these oils were not sufficient to form a clear and stable nanoemulsion. Therefore, various oils such as isopropyl myristate (IPM), oleic acid (OA), ethyl oleate (EO), Captex 200P(C-200P) and Capmul MCM(C-MCM) were screened to find the optimum ratio of oil mixture. Apart from this, other surfactants, and co-surfactants such as Transcutol P (TP), PEG-400, Tween 20 (T20), Tween 80(T80), Span 80(S80), Propylene glycol (PG), Kolliphor ELP (K-ELP) were examined for selection of an appropriate Smix ratio.

### **Selection of oil mixture**

Miscibility studies were performed using the procedure mentioned in [23] with few modifications. Mixture of 2% wt GOR and 2% wt LGE (1:1) were added to individual oil and various oil mixture (1:1) ratio, vortexed and allowed to stand for 48 hours. After 48 hours, it was examined for color change, turbidity, and phase separation. Clear and uniphasic oil mixture was selected and further studied with different surfactant mixture. Castor oil and fenugreek oil was kept constant throughout the selection procedure as they are the functional excipients.

### **Selection of surfactant mixture**

Mixture of 2% wt GOR and 2% wt LGE (1:1) was added to individual surfactant and surfactant mixture in 1:1 ratio and allowed to stand for 48 hours. After 48 hours, it was examined for colour change, turbidity and phase separation. Clear and uniphasic surfactant mixes were taken further for constructing pseudo-ternary phase diagrams.

### **Construction of pseudo-ternary phase diagram**

The nanoemulsion area was identified by the construction of pseudo-ternary phase diagrams by water titration method [24]. Based on miscibility studies, different Oilmix and Smix were selected while purified water was used as an aqueous phase. The selected surfactants and co-surfactant were mixed (Smix) in

three ratios such as 1:1 and 1:2 to identify the optimal ratio that can result in forming maximum nanoemulsion area. Briefly, the oilmix and Smix were vortexed in various ratios 9:1, 8:2, 7:3, 6:4, 5:5, 4:6, 3:7, 2:8 and 1:9 followed by drop wise water titration until phase separation or turbidity was observed. Further, the pseudoternary phase diagrams were constructed using Chemix school-Portable Chemistry software 7.0 by calculating the percent of Oilmix, Smix and water. Likewise other ratios of Smix and the zones for clear and stable nanoemulsion were identified.

## **Formulation of oil-in-water nanoemulsion**

Mixture of 1% wt GOR and 1% wt LGE was added to the selected oilmix and Smix ratios selected from the pseudo-ternary phase diagram of highest nanoemulsion region. The required amount of purified water was added dropwise with continuous stirring at ambient temperature. All the batches were stored at ambient temperature for further evaluation [25].

## **Characterization and evaluation of nanoemulsion**

### **Physical appearance, surface morphology and micromeritics (Droplet size, and polydispersity index)**

The nanoemulsion formulation was inspected visually for their colour, homogeneity and clarity. Surface morphology of nanoemulsion was studied by using Transmission Electron Microscope. The mean droplet size (MDS) is based on photon correlation spectroscopy principle, that determines the fluctuation in light scattering from Brownian movement of the particles. The MDS was determined using Zetasizer (Nano-ZS, Malvern) Instrument. The PDI ranges from 0 to 1, where 0 to 1 represents a monodisperse to polydisperse particle system. The test samples were diluted in the ratio of 1:100 using purified water. The measurements were made in 90° angle at 25°C in triplicate, mean value and standard deviation were reported [26, 27].

### **Zeta potential**

Zeta potential was determined based on the electrophoretic mobility using Zetasizer (Nano-ZS, Malvern) Instrument. It helps in predicting dispersion stability which is dependent on properties of drug, excipients concentration and presence of electrolytes. The test samples were diluted in the ratio of 1:100 using purified water [28].

### **Thermodynamic stability and Stress testing (Centrifugation, Heat-Cool cycle and Freeze-Thaw cycle)**

The optimized batches based on pseudo-ternary plots were further subjected to thermodynamic stability. The interfacial film strength was determined by testing the stability of emulsion under centrifugation. Phase separation was observed after centrifugation of the optimized formulation at 4500rpm for 20minutes. Formulations that were stable in centrifugation test, were subjected to heat-cool cycle. In heat-

cool cycle, the formulations were kept between 4°C and 45°C for six cycles for not less than 48hrs and observed visually for any physical changes. The stable formulations were further evaluated in freeze-thaw cycles. Three freeze-thaw cycles between - 21°C and + 25°C were performed at each temperature for not less than 48 hour and examined for changes in homogeneity and color [19, 29].

## **Viscosity measurements and rheological behaviour**

The viscosity of the optimized nanoemulsion was determined using Brookfield Cup and Bob Viscometer at 25°C using small sample adapter and spindle no. 63 at 150 rpm [30].

## **Degree of transparency (% transmittance)**

Transparency of nanoemulsion was evaluated by diluting at 100X and 250X with purified water and analysing the percent transmittance at 638.2 nm with purified water as blank [19].

## **Incorporation of nanoemulsion in gel system**

LGE and GOR containing nanoemulsion was o/w type of emulsion, therefore aqueous gelling agents were screened. Gelling agents such as Pemulen TR-1 NF, Carbopol 974P NF and Ultrez 10 NF were selected for preparation of nanoemulgel. Nanoemulsion was loaded in 0.5%, 0.75% and 1% wt concentration of these gelling agents. Based on viscosity, texture, and appearance 0.75% wt Ultrez-10 NF was selected in formulation of nanoemulgel. To prepare NE loaded gel, weighed amount of Ultrez 10 NF was hydrated for 2 hours in purified water (in half quantity of the aqueous phase of nanoemulsion) by stirring it on magnetic stirrer. LGE and GOR were added to oil mix, followed by addition of Smix and remaining aqueous phase. Further, nanoemulsion was then gradually added to the gel with gentle mixing to avoid excessive air entrapment. Finally, triethanolamine (TEA) was used as a pH adjusting agent to adjust the pH in the range of 5–6 in order to achieve maximum viscosity and form a homogenous, clear gel [31].

## **Evaluation and characterization of nanoemulsion loaded gel**

### **pH determination**

Topical gel must be safe and non-irritating to avoid allergic reactions. Since, pH of the formulation plays a significant role leading to allergic reactions. Hence, pH measurement of nanoemulgels is essential. Nanoemulgel pH was measured by dispersing 5 grams of gel in 50 ml of purified water (10% w/w dispersion) at 25°C using a digital pH meter calibrated at pH 4.2, 7.0 and 9.4 buffers prior to use (Labman Instruments) [32].

### **Spreadability**

1g of optimized nanoemulgel was sandwiched between two glass slides (i.e. ground slide and upper slide affixed with a hook). 200g of weight was kept for 5 min on the top to remove excess air and ensure

uniform film of the nanoemulgel. A weighed quantity (30g) was kept on pan (38gm) that was attached to the pulley. The required time (in seconds) by the glass to slip off from the nanoemulgel in the direction of certain load was recorded. The spreadability of the nanoemulgel is inversely proportional to the time required for complete separation of glass slides [33, 34]. Spreading was calculated using the mathematical formula.

$$S=m^*/l/s$$

Where  $S$  is spreadability,  $m$  is the weight placed in the pan (40g),  $l$  is the length of glass slides (10cms) and  $t$  is time required in seconds.

## Drug content determination

Ginger oleoresin consists of 6-gingerol (6-GIN) and lipid guggul extract consists of E-guggulsterone (E-GGS) and Z-guggulsterone (Z-GGS) as active drugs. The concentration of GOR and LGE in NE was determined by using RP-HPLC. 1g of NE was diluted with 10ml methanol. After appropriate dilutions with mobile phase (ACN: Methanol: water- 70:10:20) and the concentration of 6-gingerol (GOR), E and Z-guggulsterone (LGE) were determined using RP-HPLC [35].

### In-vitro diffusion study

The *in vitro* drug diffusion of optimized gel batch was determined using Franz Diffusion cell on nylon membrane of 0.45 $\mu$ m. The membrane was pre-soaked in the release media and flanked by receptor and donor compartment. The receptor compartment was filled with phosphate buffer pH 7.4: Ethanol (1:1) + 3%w/w Tween 80 (release media) in isothermal condition (37 $^{\circ}$ C  $\pm$  2 $^{\circ}$ C) and stirred magnetically at 100rpm. The aliquots were withdrawn at predetermined time intervals and quantified by the developed RP-HPLC method. The samples were replenished with fresh media after removing the aliquots. Percent cumulative drug release was calculated and plotted against time [36].

## Ex vivo diffusion study

The ex vivo drug diffusion of with optimized gel batch was performed using Franz Diffusion cell on porcine ear skin. No animals were harmed during procurement of the porcine ear skin as it was collected from a government approved abattoir. After sacrificing the animal, the membrane was pre-soaked in the release media and flanked by receptor and donor compartment. The receptor compartment was filled with release media in isothermal condition (37 $^{\circ}$ C  $\pm$  2 $^{\circ}$ C) and stirred magnetically at 100rpm. The aliquots were removed at predetermined time intervals and quantified by the developed RP-HPLC method. The samples were replenished with fresh media after removing the aliquots. Percent cumulative drug release was calculated and plotted against time. The permeation profile was constructed by calculating the quantity of drug permeated per square centimeter of skin (mcg/cm<sup>2</sup>) versus time (h). The steady state flux ( $J_{ss}$ , mcg/cm<sup>2</sup>h) was calculated from the slope of the linear portion of the plot using linear regression analysis [36–38].

## Release kinetics model

Based on the in vitro and ex vivo diffusion studies various mathematical models were applied to determine the release kinetics of the active compounds from the optimized formulation. The release data was fitted into various equation for zero order release, first order release, Higuchi release and Korsmeyer Peppas release [37].

## Differential scanning calorimetry

The change in physical properties and temperature of the optimized nanoemulsion was determined using DSC method. The sample was heated in the range of 30–500°C in an aluminum pan that was sealed with perforated lids.

## Hen's Egg Test-Chorioallantoic Membrane (HET-CAM) study

HET-CAM is a rapid and sensitive procedure to predict skin irritancy by evaluation of the changes in the CAM of the fertilized eggs. CAM comprises of complete laminate vascular system with arteries, veins and capillaries that are sensitive to harmful and corrosive substances with an inflammatory process. As per the ICCVAM-Recommended Test Method Protocol, the irritation potential of LGE + GOR formulations were evaluated by the HET- CAM assay [39]. Fertile White Leghorn chicken eggs weighing 50 to 60 grams were obtained from Central Poultry Development Organization, Mumbai. Nine-day old, fertilized eggs which were incubated in an automatic rotating machine at  $37.5 \pm 0.5^\circ\text{C}$  and  $62.5 \pm 7.5\%$  RH were utilized for the experimentation. The experimentation method was validated using 0.1 N NaOH (negative control), 0.9% NaCl (positive control and 0.75% w/w Ultrez-10 NF (gelling agent). The skin irritant property of LGE + GOR NEG was compared to LGE, GOR, LGE + GOR mixture, LGE + GOR NE and a commercial product (1.16%w/w Diclofenac emulgel). The irritating impact was observed visually for 5 minutes after 0.3ml of test solutions were applied to the CAM. The irritation score (IS) was determined using the following equation after recording the length of time and extent of injuries following the addition of each sample:

$$IS = \frac{(301 - tH) * 5}{300} + \frac{(301 - tL) * 7}{300} + \frac{(301 - tC) * 9}{300}$$

Where tH, tL and tC are time (in seconds) required for the occurrence of haemolysis, lysis and coagulation, respectively. Depending on the IS values, formulations were classified as mentioned below non-irritating ( $IS < 0.9$ ), mildly irritating ( $1.0 \leq IS \leq 4.9$ ), moderately irritating ( $5.0 \leq IS \leq 8.9$ ) or severely irritating ( $9.0 \leq IS \leq 21.0$ ). The experimentation was performed in triplicate [40, 41].

## Cytotoxicity study on RAW 264.7 cells



The in-vitro cytotoxicity study was determined by performing MTT assay in RAW 264.7 cell lines. Cells at a density of  $2 \times 10^4$  were seeded into 96-well microtiter plates (Sigma, Germany) in complete RPMI medium (200  $\mu$ L per well) and incubated at 37°C under an atmosphere of 5% CO<sub>2</sub> overnight. Cells were treated with the test compounds (GOR, LGE and LGE + GOR (1:1)) and diclofenac at 0.5  $\mu$ g/ml, 1  $\mu$ g/ml, 2  $\mu$ g/ml, 10  $\mu$ g/ml, 20  $\mu$ g/ml and 40  $\mu$ g/ml for 72hrs. This was followed by addition of 0.5 mg/mL MTT solution in each well and incubated for 3hrs at 37°C. Later, MTT solution was replaced with 100  $\mu$ L of dimethyl sulfoxide (DMSO) (Millipore sigma) for solubilizing the purple formazan crystals. The absorbance was recorded using an ELISA microplate reader (BioTek Synergy H1 Multimode Reader, USA) at  $\lambda$  max = 570 nm and 630 nm [33, 42].

## **LPS mediated anti-inflammatory study on RAW 264.7 cells**

The RAW cells were seeded at  $5 \times 10^5$  in a 6-well plate with a volume of 2ml complete RPMI 1640 medium, further it was incubated at 37°C under an atmosphere of 5% CO<sub>2</sub>. Cells were then incubated with LPS (1  $\mu$ g/ml) for 3hrs and treated with the test compounds (5% GOR, 5% LGE, 50  $\mu$ g/ml extract, 5  $\mu$ g/ml diclofenac and 2.5% each of GOR and LGE followed by incubation for 72hrs at 37°C under an atmosphere of 5% CO<sub>2</sub>. The cells were harvested in polystyrene tubes and centrifuged at 300g x g at 25°C. Cell pellets obtained by centrifugation were washed with PBS after decanting the supernatant. Cells fixation was performed by adding 1ml of cold 70% ethanol and incubated for 30min at -20°C freezer. This was followed by centrifugation and washing with PBS. 10  $\mu$ L of antibodies were added and incubated for 30min at room temperature in dark condition. 500  $\mu$ L of D-PBS was mixed thoroughly and analyzed by flow cytometer (FACS-BD Cell quest pro software) [43, 44].

## **Stability study**

Stress studies were performed by subjecting the optimized formulation at numerous temperature conditions. Formulation was packed in sealed glass containers and stored in different temperature zones at  $4 \pm 3^\circ\text{C}$ ,  $25 \pm 2^\circ\text{C}$ /  $60 \pm 5\%$  RH and  $40 \pm 2^\circ\text{C}$ /  $75 \pm 5\%$  RH for 3 months. At the end of each month the samples were aliquoted for evaluation of any physical change (such as clarity, phase separation, precipitation of API, and colour change), drug content, gelling capacity and pH [45, 46].

## **In vivo animal study**

### **Complete freund's adjuvant induced arthritic model.**

The study was carried out in the Department of Pharmacology after the approval of the protocol by the Institutional Animal Ethics Committee (IAEC) (Approval number – CPCSEA/IAEC/P-4/2020). Male Wistar Rats of 180-200g were procured from National Institute of Biosciences, Pune. Before the commencement of study, animals were acclimatized in laboratory for 2 weeks. Animals were fed with commercial pelleted diet and water *ad libitum* throughout the experimentation. Complete Freund's adjuvant (CFA) model was opted for studying the efficacy of formulated gel against anti-inflammatory condition [19].

## **Skin irritation study**

Skin irritation was performed by applying LGE + GOR NEG on wistar rats and evaluated by skin irritation. The dorsal surface of the rats were shaved without damaging the skin surface, 4 hours before the application of the respective formulation. The rats were divided into groups each containing six rats. Group1: Positive control; animals were treated as healthy controls; Group 2: animals were treated with 0.8% v/v aqueous solution of formalin; Group 3: 1.16% w/w Diclofenac emulgel; animals were treated with a commercial product; Group 4: Placebo NEG; animals were treated with nanoemulgel without drugs and Group 5: LGE + GOR NEG; animals were treated with nanoemulgel containing drugs. After application of respective formulation, they were inspected at 24, 48 and 72 hours for dermal reactions such as edema or erythema. The mean scores for recorded on the basis of severity caused by application of these formulation. 0-no erythema/edema, 1-slight erythema/edema, 2-moderate erythema/edema and 3-severe erythema/edema.

## **Paw edema measurement**

The paw edema was measured using digital Vernier caliper on day 0, 7th, 14th, 21st and 28th day. Paw edema changes were determined by measuring the difference in paw (in mm) between the initial day and the predetermined days (0, 7th, 14th, 21st and 28th day).

## **X ray analysis**

Animals were euthanized on the 28th day and the left hind paws were cut and stored in neutral buffer containing 10% formalin solution. Later, the severity joint and bone deformation were analyzed.

## **Histopathological analysis**

After euthanizing animals, left hind paw was stored in neutral buffer with 10% formalin solution. Joint tissue section were sliced into 5  $\mu$ m segments and placed on a glass slide followed by staining using haematoxylin and eosin (H&E) sections. Further the sections were analyzed for cell infiltration, cartilage damage and bone erosion.

## **Plasma and synovium IL-6, IL-10 and TNF- $\alpha$ measurements**

Blood serum and synovial fluid were collected after the last administration of formulation. Cytokines level of TNF- $\alpha$ , IL-6 and IL-10 were determined using ELIZA kit [47, 48].

## **Statistical analysis**

One-way analysis of variance (ANOVA) was applied to determine the statistical difference. Cell cytotoxicity was analyzed using the student's t-test with a 95% confidence interval. For all statistical analyses, Graph Pad Prism version 7.0 (GraphPad Software, San Diego, California USA) was used.

## Results and Discussion

### Selection of oils, surfactants, and co-surfactants

Miscibility studies were carried out to select the most suitable oil phase and aqueous phase. The miscibility of ginger oil and lipid guggul extract was determined by mixing with various oils. Castor oil and fenugreek oil were selected as the functional excipients. The results of the miscibility studies suggest 4% wt drug mixture (1:1) was completely miscible in all the individual as well as oil mixture. The combination of oil mentioned in Table 1 had the highest emulsification ability. The ratio of castor oil and fenugreek oil to other oils was kept 0.5:0.5:1:1 as increasing its concentration led to instability and turbidity in the system. Similarly, the following ratio of surfactant and cosurfactant, mentioned in Table 2 were used for the development of nanoemulsion.

Table 1  
List of selected Oilmix based on miscibility.

Selected Oilmix	Composition	Ratio
O-1	CO: FO: OA: C-200 P	0.5: 0.5: 1: 1
O-2	CO: FO: OA: C-MCM	0.5: 0.5: 1: 1
O-3	CO: FO: EO: C-200 P	0.5: 0.5: 1: 1
O-4	CO: FO: EO: C-MCM	0.5: 0.5: 1: 1

Table 2  
List of selected Smix based on of miscibility.

Selected Smix	Composition	Ratio
S-1	T-80: K-ELP: TP	1: 1: 1
S-1A	T-80: K-ELP: TP	0.5:0.5:1
S-2	T-80: K-ELP: PEG-400	1: 1: 1
S-2A	T-80: K-ELP: PEG-400	0.5:0.5:1
S-3	T-80: K-ELP: PG	1: 1: 1
S-3A	T-80: K-ELP: PG	0.5:0.5:1

## Formulation and development

Formulation of nanoemulsion was carried out using pseudoternary phase diagrams. Construction of the pseudoternary diagram is important for determining the concentration of each component to form a stable NE system. Pseudo ternary diagrams were constructed from the selected Oilmix and Smix (mentioned in Table 3) to identify the o/w nanoemulsion region. The pseudo ternary diagrams with various weight ratios of Smix (0.5:0.5:1 and 1:1:1) were constructed, whilst keeping the oilmix ratios constant as shown in Fig. 1. Pseudoternary diagrams indicated low area for nanoemulsion in oilmix containing CO, FO, OA and C-200P compared to nanoemulsion region of oilmix containing CO:FO: OA:C-MCM and CO:FO: EO:C-MCM. The Smix contained surfactants in different ratios (0.5:0.5:1 and 1:1:1), however the phase diagrams didn't show any significant difference in the nanoemulsion region. The nanoemulsion batches were formulated depending on the nanoemulsion region from the phase diagrams. Based on the pseudoternary, different batches of nanoemulsion were developed and depending on the observation 6 batches were selected for further characterization and development. Trial batches of nanoemulsion containing 2% w/w is illustrated in Table 4.

Table 3  
List of selected Oilmix and S mix combinations for Pseudo ternary phase diagrams

<b>Ternary No</b>	<b>Oilmix</b>	<b>Smix</b>
1	O-1: CO: FO: OA: C-200 P (0.5:0.5:1:1)	S-2A: T-80: K-ELP: PEG-400 (0.5:0.5:1)
2	O-2: CO: FO: OA: C-MCM (0.5:0.5:1:1)	S-3A: T-80: K-ELP: PG (0.5:0.5:1)
3	O-3: CO: FO: EO: C-200 P (0.5:0.5:1:1)	S-2A: T-80: K-ELP: P-400 (0.5:0.5:1)
4	O-4: CO: FO: EO: C-MCM (0.5:0.5:1:1)	S-1A: T-80: K-ELP: TP (0.5:0.5:1)
5	O4: CO: FO: EO: C-MCM (0.5:0.5:1:1)	S-2A: T-80: K-ELP: PEG-400 (0.5:0.5:1)
6	O-1: CO: FO: OA: C-200 P (0.5:0.5:1:1)	S-1B: T-80: K-ELP: TP (1:1:1)
7	O-2: CO: FO: OA: C-MCM (0.5:0.5:1:1)	S-3B: T-80: K-ELP: PG (1:1:1)

## Droplet size, polydispersity index and zeta potential

The mean globule size of all the nanoemulsion was found to be between  $18.03 \pm 2.55$ nm to  $72.56 \pm 54.56$  nm and PDI was below 0.4 (shown in Fig. 2). For topical drug delivery, the ideal mean globule size is less than 200 nm, with a PDI less than 1.0. Smaller the mean globule size, larger is the surface area which is

suitable for rapid pore transport. Zeta potential is an indication of surface charges which contributes in providing stability of the formulation. All the nanoemulsion prepared had a negative zeta potential in the range of -8 to -23 mV indicating their ability to avoid agglomeration and maintain interfacial boundary of the globules resulting into enhanced stability of nanoemulsion. The results of droplet size, PDI and ZP has been highlighted in Table 5. Also, the TEM image of the developed nanoemulsion is shown in Fig. 3.

Table 4  
Trail batches containing 2% w/w Drug mixture (1:1)

Batch No	Oil (%)	Surfactant (%)	Millipore Water (%)	Observation
1	O-2 10	S-5A 40	48	Clear
2	O-3 10	S-4A 45	43	Clear
3	O-4 10	S-1A 50	38	Clear
4	O-4 10	S-4A 40	48	Clear
5	O-1 5	S-1B 45	48	Clear
6	O-2 10	S-5B 40	48	Clear

## Thermodynamic stability and %Transmittance

The formulated batches were further investigated for thermodynamic stability by performing centrifugation, heat-cool cycle and freeze-thaw cycle. The results are shown in Table 5. The batches were found to be thermodynamically stable as they could withstand centrifugation, heat-cool cycle and freeze-thaw cycle. Percentage transmittance of nanoemulsion was found to be between  $95.77 \pm 0.05\%$  to  $99.54 \pm 0.19\%$  at 100X dilution and more than 99.49 at 250X dilution.

Table 5  
Characterization of nanoemulsion batches

Batch No	Zeta size (nm)	PDI	Zeta Potential (mV)	% Transmittance		Thermodynamic stability		
				100 X	250X	Centrifugation	Heat-Cool	Freeze-Thaw
1	21.41 ± 0.02	0.269 ± 0.008	-15.1 ± 0.24	98.47	98.47	Passed	Passed	Passed
2	20.67 ± 0.02	0.153 ± 0.01	-12.5 ± 0.48	99.544	99.944	Passed	Passed	Passed
3	25.39 ± 0.04	0.342 ± 0.007	-14.7 ± 0.22	95.177	101.132	Passed	Passed	Passed
4	22.73 ± 0.02	0.220 ± 0.06	-18.1 ± 0.11	97.789	101.102	Passed	Passed	Passed
5	23.76 ± 54.5	0.632 ± 0.05	-15 ± 0.21	97.526	100.941	Passed	Passed	Passed
6	16.08 ± 2.55	0.187 ± 0.06	-22.4 ± 0.31	96.51	99.974	Passed	Passed	Passed

## Incorporation of nanoemulsion in gel system

Nanoemulsion was further incorporated into various carbopol gel system such as 0.5%, 0.75% and 1% wt Carbopol 974P NF, Ultrez-10 NF and Pemulen TR-1 respectively. Formulation with Carbopol 974P were viscous but were least clear (turbid) as compared to the other gelling agents. On the other hand, formulation with Pemulen TR-1 had a gritty texture and less viscosity as compared to Ultrez-10 NF. Formulation with Ultrez-10 NF were clear and homogeneous but 0.75% wt Ultrez-10 NF had the optimum viscosity along with clarity and homogeneity, it was selected as the gelling agent.

Table 6  
Characterization of nanoemulgel

Batch No	pH (n = 3)	Spreadability (g.cm/s)	Viscosity (cps)	% Drug content in nanoemulgel		
				6-gingerol	E-GGS	Z-GGS
1	5.46 ± 0.02	18.7 ± 1.32	32.86 ± 0.41	107.27 ± 2.47	90.69 ± 3.68	98.06 ± 1.17
2	5.20 ± 0.03	19.87 ± 1.07	35.8 ± 1.46	97.64 ± 1.25	100.99 ± 2.11	107.1 ± 2.74
3	5.42 ± 0.02	21.4 ± 1.54	36.3 ± 0.1	101.72 ± 1.96	92.45 ± 5.48	99.32 ± 3.18
4	5.53 ± 0.05	17.2 ± 0.98	39.7 ± 0.98	108.36 ± 3.98	96.34 ± 3.77	94.67 ± 2.96
5	5.48 ± 0.03	17.63 ± 2.47	35.63 ± 6.82	97.92 ± 2.51	98.74 ± 2.21	104.26 ± 2.65
6	5.34 ± 0.04	22.41 ± 1.71	38.8 ± 3.21	105.28 ± 4.78	103.50 ± 2.16	94.32 ± 3.14
7	5.53 ± 0.01	25.4 ± 1.21	35.63 ± 1.75	98.90 ± 2.27	101.13 ± 1.25	106.49 ± 0.98

## Determination of pH, viscosity, spreadability and drug content

The mean pH of the drug loaded nanoemulgel were 5–6 (slightly acidic) which indicates compatibility of the gels with the skin surface i.e., no skin irritation or inflammation is expected with skin. Spreadability measurements were performed based on the slip and drag characteristics of the nanoemulgel, which is an indirect method to determine the gel's uniform spreadability and applicability on the skin. The spreadability of all formulation was between 17 to 26 g.cm/s. The viscosity of all the developed batches is highlighted in Table 6. The drug content of all the selected nanoemulsion batches were found to be within the range of 90–110%. The drug content in batch 6 was found to be 105.28 ± 4.78, 103.50 ± 2.14 and 94.32 ± 3.14 of 6-gingerol, E-GGS and Z-GGS respectively.

## In vitro diffusion study

In vitro diffusion study of batch 6 loaded gel was performed in release media using Franz diffusion cell using nylon membrane (0.45µm). At 24th hour, (Fig. 4a) around 99.72 ± 3.47%, 57.98 ± 2.11% and 86.42 ± 5.13% of 6-GIN, E-GGS and Z-GGS respectively were released from the gel matrix. However, in the case of nanoemulsion the release was faster and at 8th hour around 80% of the drug was release. Therefore, it can be stated that incorporation of nanoemulsion in gel matrix ensures controlled drug delivery.

## Ex vivo diffusion study

Ex vivo diffusion study of Batch no. 6 loaded gel (1 gram) was performed in release media using Franz diffusion cell using porcine ear skin as membrane. At 24th hour, around  $92.8 \pm 3.21\%$ ,  $55.61 \pm 0.91\%$  and  $84.2 \pm 4.22\%$  of 6-GIN, E-GGS and Z-GGS respectively was released from the gel matrix. In ex vivo study, % drug diffused was found to be less as compared to in vitro drug diffusion which can be attributed to presence of fatty layer in porcine ear. The graphical representation of ex vivo diffusion study is shown in Fig. 4b. The permeation coefficient of 6-GIN, E-GGS and Z-GGS was found to be  $0.233\text{cm}^2/\text{hr}$ ,  $0.135\text{cm}^2/\text{hr}$  and  $0.201\text{cm}^2/\text{hr}$  respectively.

## Release kinetics model

Drug release kinetics and drug permeation mechanism from the optimised GOR + LGE NE loaded gel were analyzed using kinetic models such as zero order, first order, Higuchi model, and Korsmeyer-Peppas. In the case of in vitro drug diffusion, overall curve fitting showed Korsmeyer-peppas with  $R^2$  of 0.8790 for GOR (6-GIN), 0.9669 and 0.9868 for LGE (E-GGS and Z-GGS) respectively. Based on the  $R^2$  value the types of release kinetic is identified. In case of ex vivo drug diffusion, overall curve fitting showed Korsmeyer-peppas with  $R^2$  of 0.8743 for GOR (6-GIN), 0.9582 and 0.9855 for LGE (E-GGS and Z-GGS) respectively. Table 7 represents the regression coefficient for in vitro and ex vivo drug diffusion. It was observed that the GOR has Korsmeyer-Peppas type of release kinetics, whereas LGE showed zero order release. These results suggests that the drug show release in controlled manner.

Table 7  
Release kinetic for optimized nanoemulgel in in vitro and ex vivo drug diffusion study

		6-GIN (R <sup>2</sup> )	E-GGS (R <sup>2</sup> )	Z-GGS (R <sup>2</sup> )
In vitro drug diffusion	Zero order	0.7813	0.9669	0.9868
	First order	0.831	0.8104	0.7656
	Higuchi	0.8605	0.8064	0.8491
	Korsmeyer-Peppas	0.879	0.9692	0.9032
Ex vivo drug diffusion	Zero order	0.7745	0.9582	0.9855
	First order	0.831	0.8136	0.7665
	Higuchi	0.8512	0.789	0.8455
	Korsmeyer-Peppas	0.8743	0.9883	0.9083

## Differential Scanning Colorimetry



DSC thermogram of gingerol, lipid guggul extract and mixture of gingerol and lipid guggul extract is shown in Fig. 5a, 5b and 5c. As per the DSC thermograms, GOR and LGE shows exothermic peaks at 383.0°C and 392.5°C respectively. Figure 5c shows endothermic peaks at 389.7°C and 400.3°C which corresponds to peaks of GOR and LGE respectively. Figure 5f indicates the DSC overlay which does not show the presence of endothermic peak of both drugs and was identical to the thermogram of placebo nanoemulsion. Therefore, it can be concluded that the drug was completely encapsulated in the lipidic phase.

## Hen's Egg Test-Chorioallantonic Membrane (HET-CAM) study

As mentioned in Table 8 and shown in Fig. 6 the nanoemulgel was found to be non-irritating and non-sensitizing in nature as compared to pure drugs, conventional gel and marketed formulation (diclofenac emulgel) which has slight irritation potential. This suggests that encapsulation of these drug in nanocarriers such as nanomemulsion could be an effective way to reduce skin irritation possessed by pure extracts.

## Stability study

The final formulation was charged for stability for 3 months and then evaluated with respect to physical appearance, pH, globule size, zeta potential and drug content. The results mentioned in Table 9 indicates that the formulation is stable. Also, the variations in evaluated parameters indicated the results were not statistically significant ( $p > 0.05$ ).

Table 8  
Comparative evaluation of various formulation w.r.t level of skin irritation

Compounds	IS Score (mean $\pm$ SD)	Irritation level
Negative control (0.9% NaCl)	0.00	No Irritation
Positive control (0.1N NaOH)	11.996 $\pm$ 0.00096	Severe Irritation
Vehicle (Olive oil)	0.00	No Irritation
0.75% Carbopol Ultrez 10 NF	0.00	No Irritation
1% LGE solution	2.144 $\pm$ 0.1456	Slight Irritation
1% GOR solution	6.51 $\pm$ 0.0467	Moderate Irritation
1%LGE + 1% GOR solution	7.088 $\pm$ 0.116	Moderate Irritation
Placebo NEG	0.00	No Irritation
1% LGE + 1% GOR NEG	0.00	No Irritation
1.16% w/w Diclofenac sodium Emulgel	3.118 $\pm$ 0.0486	Slight Irritation

## Cytotoxicity study on RAW 264.7 cells

Figure 7 shows % cell viability of 25% GOR, LGE, LGE + GOR and diclofenac on RAW 264.7 cells. The results of MTT assay suggests that the IC<sub>50</sub> values of 25% GOR, LGE, LGE + GOR and diclofenac on RAW 264.7 cells were  $39.06 \pm 0.34$ ,  $36.1 \pm 0.55\%$ ,  $19.74 \pm 0.13$  and  $36.73 \mu\text{g/ml}$  respectively.

## LPS mediated anti-inflammatory study on RAW 264.7 cells

LPS mediated anti-inflammatory studies were performed on RAW 264.7 cells to determine the levels of cytokines IL-6, IL-10 and TNF- $\alpha$ . Figure 8 depicts % of cells stimulated with LPS expressing the cytokines IL-6, IL-10 and TNF- $\alpha$  after treating with various test compounds. LPS induced cells treated with either GOR or LGE did not showed improvement in the expression of cytokine level. It is evident from the graph that treatment with GOR and LGE expressed cytokines similar to diclofenac. Also, the cells treated with GOR-LGE NEG showed significant decrease in the levels of anti-inflammatory cytokines IL-6 and TNF- $\alpha$  and increase in pro-inflammatory cytokine IL-10. Therefore, it can be stated that the combination of LGE and GOR incorporated into nanoemulsion can be used for the treatment in reducing the anti-inflammatory activity.

Table 9  
Three months stability study data

Sr. no	Parameter	Day 0	After 3 months			
			At 4°C	At ambient temperature	At 45°C	
1	Physical appearance	Yellow & clear	Yellow & clear	Yellow & clear	Yellow & clear	
2	pH	$5.34 \pm 0.02$	$5.34 \pm 0.01$	$5.32 \pm 0.03$	$5.36 \pm 0.02$	
3	Globule size	$18.03 \pm 2.55$	$18.98 \pm 3.49$	$18.20 \pm 2.43$	$19.12 \pm 2.87$	
4	Zeta potential	$-22.4 \pm 5.75$	$-20.2 \pm 4.62$	$-21.60 \pm 2.87$	$-18.2 \pm 7.86$	
5	(%) Drug content	6-GIN	105.28	104.12	105.12	103.21
	(%) Drug content	E-GGS	103.5	102.87	103.37	102.36
	(%) Drug content	Z-GGS	99.32	99.06	99.08	98.36

## **Complete Freund's Adjuvant Induced arthritis model**

On Day 0, 0.1 ml of CFA was injected into the left hind paw's sub plantar region to cause RA in wistar rats. The ankle width measurements were conducted prior and after 24 hours of induction. Paw edema and body weight was monitored on a weekly basis i.e on day 1, 7, 14, 21 and 28 day of the induction. Blood withdrawal was done on day 28 for TNF- $\alpha$ , IL-6 and IL -10 estimation in rat blood plasma. Paw was separated from the animal for X –ray and histopathological analysis after sacrificing them.

## **Skin irritation studies**

The topical application should be free from skin irritation and sensitivity reactions. In this, it was observed that LGE and GOR loaded nanoemulgel did not show any severe skin irritation.

symptoms such as edema and erythema during 72 hrs of observation as compared to diclofenac emulgel which showed slight irritation of skin. Therefore, it was concluded that the optimized nanoemulgel is non-irritating, non-sensitizing and safe for topical use.

## **Paw edema measurement**

The measurement of the paw edema was done using digital vernier caliper. Paw edema measured on Day1, 7, 14, 21 and 28 (shown in Fig. 9) indicated that LGE + LGE NEG and diclofenac sodium emulgel showed significant reduction in the edema on 28th day after the treatment as compared to positive and Placebo LEG groups.

## **X-ray analysis**

Radiographic examination of the paw from positive control group (shown in Fig. 10) showed the normal joint without distension and normal joint space radio density. Animals from negative control and placebo nanoemulgel group showed arthritic changes such as increase joint radio density and narrowing in joint space were observed. However, the severity and intensity were reduced in the LGE + GOR NEG group and Diclofenac Na emulgel group. The joint space and radio density were comparable between Diclofenac emulgel group and LGE + GOR NEG group suggestive of good anti-inflammatory and anti-arthritic properties.

## **Histopathology study**

In fig no. 11, microscopic examination of paw showed normal bone tissue in the positive control group of animals. Animals from negative control and placebo nanoemulgel showed inflammatory changes such as infiltration of inflammatory cells and minimal erosion in bone when compared with control group. However, animals from group Diclofenac Na emulgel, and LGE + GOR nanoemulgel showed decreased in the severity of inflammatory cells. Based on histopathology findings, it can be concluded animal treated with Diclofenac Na emulgel and LGE + GOR nanoemulgel showed decreased in the severity and incidence of these changes indicating of anti-arthritic effects.

# Estimation of IL-6, TNF- $\alpha$ & IL-10 in blood plasma and synovium

IL-6 and TNF- $\alpha$  are anti-inflammatory cytokine prominently present during the progression of RA. It was observed that LGE + GOR NEG and diclofenac sodium emulgel reduced the IL-6 and TNF- $\alpha$  levels more than the positive and placebo NEG in plasma and synovium. Similar results were observed with pro-inflammatory cytokine IL-10. The graphical representation of the data has been shown in Fig. 12. Therefore, LGE + GOR NEG can be used as an effective alternative for management of pain and inflammation associated to rheumatoid arthritis.

## Conclusion

In conclusion, the present work was focused to develop GOR and LGE nanoemulgel for the treatment for rheumatoid arthritis. In vitro studies suggested that drug loaded nanoemulgel exhibited a slow and prolonged release of the both drugs. Based on HET-CAM, it can be stated that the formed nanoemulgel had no skin irritation ability as compared to diclofenac emulgel which showed slight irritation in both the study. Therefore, nanoemulsion can be an efficient technique in encapsulating the drug with irritating potential. During the preclinical studies, it was observed that drug loaded nanoemulgel had better efficacy in terms of reduction of inflammation of the paw edema which was supported by histopathological and X-ray analysis. IL-6 and TNF- $\alpha$  levels in plasma were found to reduce and the levels of IL-10 in drug loaded nanoemulgel and diclofenac emulgel. Therefore, ginger oleoresin and lipid guggul extract based nanoemulgel can be potential candidate for further studies as a new efficient treatment in patients with Rheumatoid Arthritis.

## Declarations

**Ethics approval:** Animal study protocol was approved by the Institutional Animal Ethics Committee (IAEC) (Approval number – CPCSEA/IAEC/P-4/2020).

**Consent for publication:** Yes

**Competing interests:** The authors declare no competing interests.

**Funding** We thank Rajiv Gandhi Science & Technology Commission (RGSTC) for providing funding for this project (RGSTC/File-2017/DPP-175/CR-30).

**Author contribution** All authors contributed to study conception and design, material preparation, data collection, analysis and drafting of manuscript.

**Acknowledgments:** None

## References

1. Guo Q, Wang Y, Xu D, Nossent J, Pavlos NJ, Xu J. Rheumatoid arthritis: pathological mechanisms and modern pharmacologic therapies. *Bone Res.* 2018;6:15.
2. Kemble S, Croft AP. Critical Role of Synovial Tissue–Resident Macrophage and Fibroblast Subsets in the Persistence of Joint Inflammation. *Front Immunol.* 2021;12:715894.
3. Anita C, Munira M, Mural Q, Shaily L. Topical nanocarriers for management of Rheumatoid Arthritis: A review. *Biomedicine & Pharmacotherapy.* 2021;141:111880.
4. Almoallim H, Al Saleh J, Badsha H, Ahmed HM, Habjoka S, Menassa JA, et al. A Review of the Prevalence and Unmet Needs in the Management of Rheumatoid Arthritis in Africa and the Middle East. *Rheumatol Ther.* 2021;8:1–16.
5. Nilsson J, Andersson M, Hafström I, Svensson B, Forslind K, Ajeganova S, et al. Influence of Age and Sex on Disease Course and Treatment in Rheumatoid Arthritis. *OARRR.* 2021;Volume 13:123–38.
6. Saxena A, Raychaudhuri SK, Raychaudhuri SP. Rheumatoid Arthritis: Disease Pathophysiology. Inflammation, Advancing Age and Nutrition: Research and Clinical Interventions. 2013;215–29.
7. Shehu S, Kurya AU, Aliyu U, Sharma DC. Role of Inflammatory Cytokines in the Pathogenesis of Rheumatoid Arthritis and Novel Therapeutic Targets.
8. Deane KD, Holers VM. Rheumatoid Arthritis Pathogenesis, Prediction, and Prevention: An Emerging Paradigm Shift. *Arthritis Rheumatol.* 2021;73:181–93.
9. Gómez-Bañuelos E, Mukherjee A, Darrah E, Andrade F. Rheumatoid Arthritis-Associated Mechanisms of *Porphyromonas gingivalis* and *Aggregatibacter actinomycetemcomitans*. *JCM.* 2019;8:1309.
10. Köhler, Günther, Kaudewitz, Lorenz. Current Therapeutic Options in the Treatment of Rheumatoid Arthritis. *JCM.* 2019;8:938.
11. Lindler BN, Long KE, Taylor NA, Lei W. Use of Herbal Medications for Treatment of Osteoarthritis and Rheumatoid Arthritis. *Medicines.* 2020;7:67.
12. Ballester P, Cerdá B, Arcusa R, Marhuenda J, Yamedjeu K, Zafrilla P. Effect of Ginger on Inflammatory Diseases. *Molecules.* 2022;27:7223.
13. Jayanudin, Fahrurrozi Moh, Wirawan SK, Rochmadi. Preparation of Chitosan Microcapsules Containing Red Ginger Oleoresin Using Emulsion Crosslinking Method. *Journal of Applied Biomaterials & Functional Materials.* 2019;17:228080001880991.
14. Bhardwaj M, Alia A. *Commiphora wightii* (Arn.) Bhandari. Review of Its Botany, Medicinal Uses, Pharmacological Activities and Phytochemistry. *J Drug Delivery Ther.* 2019;9:613–21.
15. Bhat MH, Fayaz M, Kumar A, Jain AK. Chemistry and Pharmacology of Guggulsterone: An Active Principle of Guggul Plant. In: Ozturk M, Hakeem KR, editors. *Plant and Human Health, Volume 3* [Internet]. Cham: Springer International Publishing; 2019 [cited 2023 Apr 7]. p. 301–19. Available from: [http://link.springer.com/10.1007/978-3-030-04408-4\\_14](http://link.springer.com/10.1007/978-3-030-04408-4_14)
16. Arianto A, Cindy C. Preparation and Evaluation of Sunflower Oil Nanoemulsion As a Sunscreen. *Open Access Maced J Med Sci.* 2019;7:3757–61.

17. Bashir M, Ahmad J, Asif M, Khan S-U-D, Irfan M, Y Ibrahim A, et al. Nanoemulgel, an Innovative Carrier for Diflunisal Topical Delivery with Profound Anti-Inflammatory Effect: in vitro and in vivo Evaluation. *IJN*. 2021;Volume 16:1457–72.
18. Basudkar V, Gharat SA, Momin MM, Shringarpure M. A Review of Anti-Aging Nanoformulations: Recent Developments in Excipients for Nanocosmeceuticals and Regulatory Guidelines. *Crit Rev Ther Drug Carrier Syst*. 2022;39:45–97.
19. Gokhale JP, Mahajan HS, Surana SJ. Quercetin loaded nanoemulsion-based gel for rheumatoid arthritis: In vivo and in vitro studies. *Biomedicine & Pharmacotherapy*. 2019;112:108622.
20. Sharma B, Iqbal B, Kumar S, Ali J, Baboota S. Resveratrol-loaded nanoemulsion gel system to ameliorate UV-induced oxidative skin damage: from in vitro to in vivo investigation of antioxidant activity enhancement. *Arch Dermatol Res*. 2019;311:773–93.
21. G S, G. L. S, Pushpan CK, Nambisan B, A H. Evaluation of anti-arthritic potential of *Trigonella foenum graecum* L. (Fenugreek) mucilage against rheumatoid arthritis. *Prostaglandins & Other Lipid Mediators*. 2018;138:48–53.
22. Ladani M. Brief review on analgesic and anti-inflammatory properties of *Moringa oleifera*, *Senna auriculata* & other useful medicinal plants to inhibit release of immune mediators. *International Journal of Herbal Medicine*. 2022;10.
23. Kheawfu K, Pikulkaew S, Rades T, Müllertz A, Okonogi S. Development and characterization of clove oil nanoemulsions and self-microemulsifying drug delivery systems. *Journal of Drug Delivery Science and Technology*. 2018;46:330–8.
24. Sharma P, Tailang M. Design, optimization, and evaluation of hydrogel of primaquine loaded nanoemulsion for malaria therapy. *Futur J Pharm Sci*. 2020;6:26.
25. Arora R, Aggarwal G, Harikumar SL, Kaur K. Nanoemulsion Based Hydrogel for Enhanced Transdermal Delivery of Ketoprofen. *Advances in Pharmaceutics*. 2014;2014:1–12.
26. Mohammed NK, Muhialdin BJ, Meor Hussin AS. Characterization of nanoemulsion of *Nigella sativa* oil and its application in ice cream. *Food Sci Nutr*. 2020;8:2608–18.
27. Pathan I, Mangle M, Bairagi S. Design and Characterization of Nanoemulsion for Transdermal Delivery of Meloxicam. *Analytical Chemistry Letters*. 2016;6:286–95.
28. Sharma N, Kaur G, Khatkar SK. Optimization of emulsification conditions for designing ultrasound assisted curcumin loaded nanoemulsion: Characterization, antioxidant assay and release kinetics. *LWT*. 2021;141:110962.
29. Donthi MR, Saha RN, Singhvi G, Dubey SK. Dasatinib-Loaded Topical Nano-Emulgel for Rheumatoid Arthritis: Formulation Design and Optimization by QbD, In Vitro, Ex Vivo, and In Vivo Evaluation. *Pharmaceutics*. 2023;15:736.
30. Pereira Oliveira CN, Nani Leite M, de Paula NA, Araújo Martins Y, Figueiredo SA, Cipriani Frade MA, et al. Nanoemulsions Based on Sunflower and Rosehip Oils: The Impact of Natural and Synthetic Stabilizers on Skin Penetration and an Ex Vivo Wound Healing Model. *Pharmaceutics*. 2023;15:999.

31. Lala RR, Awari NG. Nanoemulsion-based gel formulations of COX-2 inhibitors for enhanced efficacy in inflammatory conditions. *Appl Nanosci.* 2014;4:143–51.
32. Gostyńska A, Czerniel J, Kuźmińska J, Brzozowski J, Majchrzak-Celińska A, Krajka-Kuźniak V, et al. Honokiol-Loaded Nanoemulsion for Glioblastoma Treatment: Statistical Optimization, Physicochemical Characterization, and an In Vitro Toxicity Assay. *Pharmaceutics.* 2023;15:448.
33. Gharat S, Basudkar V, Momin M, Prabhu A. Mucoadhesive Oro-Gel–Containing Chitosan Lipidic Nanoparticles for the Management of Oral Squamous Cell Carcinoma. *J Pharm Innov [Internet].* 2023 [cited 2023 Apr 7]; Available from: <https://link.springer.com/10.1007/s12247-023-09724-7>
34. Mutimer MN, Riffkin C, Hill JA, Glickman ME, Cyr GN. Modern Ointment Base Technology II.:Comparative Evaluation of Bases\*. *Journal of the American Pharmaceutical Association (Scientific ed).* 1956;45:212–8.
35. Latif MS, Nawaz A, Asmari M, Uddin J, Ullah H, Ahmad S. Formulation Development and In Vitro/In Vivo Characterization of Methotrexate-Loaded Nanoemulsion Gel Formulations for Enhanced Topical Delivery. *Gels.* 2022;9:3.
36. Algahtani MS, Ahmad MZ, Ahmad J. Nanoemulgel for Improved Topical Delivery of Retinyl Palmitate: Formulation Design and Stability Evaluation. *Nanomaterials.* 2020;10:848.
37. Morsy, Abdel-Latif, Nair, Venugopala, Ahmed, Elsewedy, et al. Preparation and Evaluation of Atorvastatin-Loaded Nanoemulgel on Wound-Healing Efficacy. *Pharmaceutics.* 2019;11:609.
38. Nagaraja S, Basavarajappa GM, Attimarad M, Pund S. Topical Nanoemulgel for the Treatment of Skin Cancer: Proof-of-Technology. *Pharmaceutics.* 2021;13:902.
39. Interagency Coordinating Committee on the Validation of Alternative Methods (ICCVAM). Recommended Test Method Protocol: Hen ' s Egg Test – Chorioallantoic Membrane ( HET-CAM ) Test Method. ICCVAM Test Method Evaluation Report. 2010;13:B30–8.
40. Alvarez-Rivera F, Fernández-Villanueva D, Concheiro A, Alvarez-Lorenzo C.  $\alpha$ -Lipoic Acid in Soluplus® Polymeric Nanomicelles for Ocular Treatment of Diabetes-Associated Corneal Diseases. *Journal of Pharmaceutical Sciences.* 2016;105:2855–63.
41. Anantaworasakul P, Chaiyana W, Michniak-Kohn BB, Rungseewijitprapa W, Ampasavate C. Enhanced Transdermal Delivery of Concentrated Capsaicin from Chili Extract-Loaded Lipid Nanoparticles with Reduced Skin Irritation. *Pharmaceutics.* 2020;12:463.
42. Suresh P, Salem-Bekhit MM, Veedu HP, Alshehri S, Nair SC, Bukhari SI, et al. Development of a Novel Methotrexate-Loaded Nanoemulsion for Rheumatoid Arthritis Treatment with Site-Specific Targeting Subcutaneous Delivery. *Nanomaterials.* 2022;12:1299.
43. Qiu J-G, Mei X-L, Chen Z-S, Shi Z. Cytokine Detection by Flow Cytometry. In: Vancurova I, editor. *Cytokine Bioassays [Internet].* New York, NY: Springer New York; 2014 [cited 2023 Apr 8]. p. 235–42. Available from: [https://link.springer.com/10.1007/978-1-4939-0928-5\\_21](https://link.springer.com/10.1007/978-1-4939-0928-5_21)
44. Soni JM, Sardoiwala MN, Choudhury SR, Sharma SS, Karmakar S. Melatonin-loaded chitosan nanoparticles endows nitric oxide synthase 2 mediated anti-inflammatory activity in inflammatory bowel disease model. *Materials Science and Engineering: C.* 2021;124:112038.

45. Rehman A, Iqbal M, Khan BA, Khan MK, Huwaimel B, Alshehri S, et al. Fabrication, In Vitro, and In Vivo Assessment of Eucalyptol-Loaded Nanoemulgel as a Novel Paradigm for Wound Healing. *Pharmaceutics*. 2022;14:1971.
46. Sultan MH, Javed S, Madkhali OA, Alam MI, Almoshari Y, Bakkari MA, et al. Development and Optimization of Methylcellulose-Based Nanoemulgel Loaded with Nigella sativa Oil for Oral Health Management: Quadratic Model Approach. *Molecules*. 2022;27:1796.
47. Kimmerling KA, Gomoll AH, Farr J, Mowry KC. Amniotic Suspension Allograft Modulates Inflammation in a Rat Pain Model of Osteoarthritis. *J Orthop Res*. 2020;38:1141–9.
48. Pandey S, Rai N, Mahtab A, Mittal D, Ahmad FJ, Sandal N, et al. Hyaluronate-functionalized hydroxyapatite nanoparticles laden with methotrexate and teriflunomide for the treatment of rheumatoid arthritis. *International Journal of Biological Macromolecules*. 2021;171:502–13.

## Figures

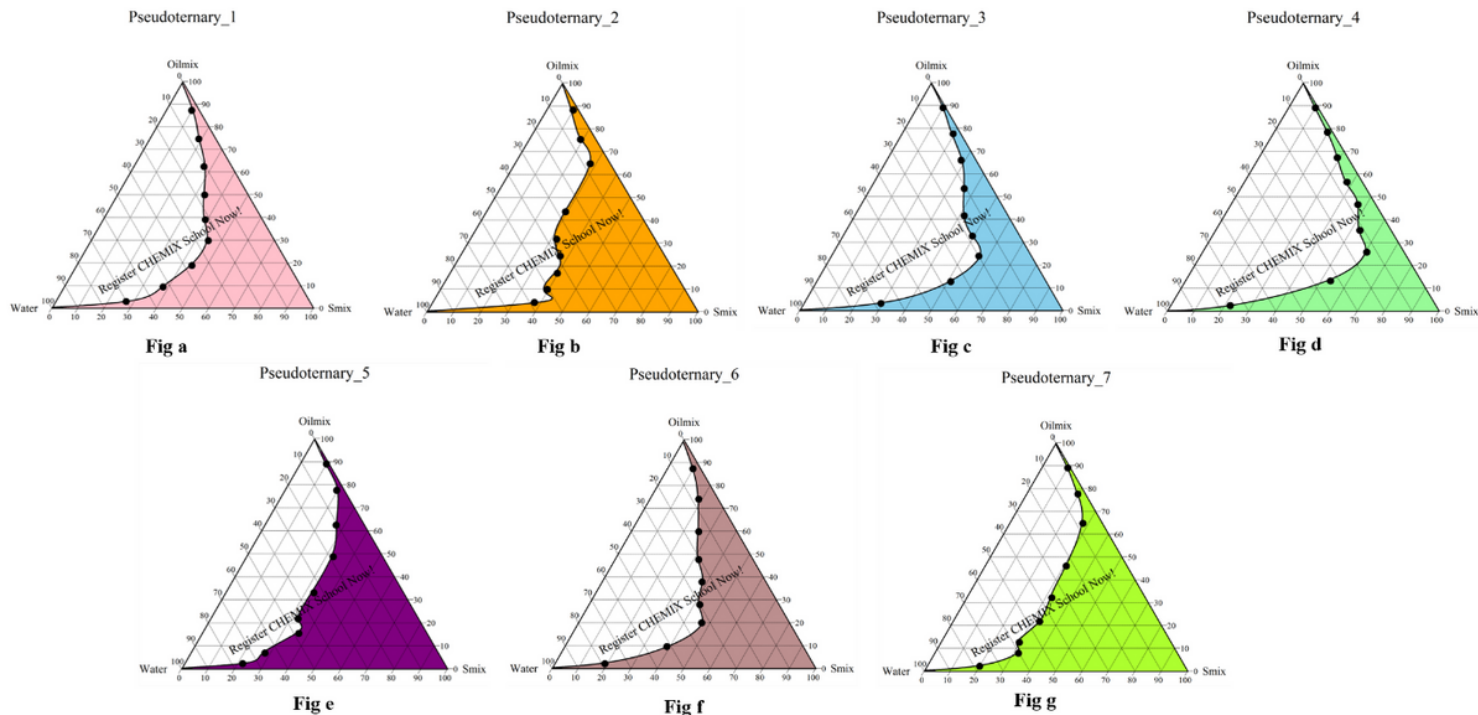
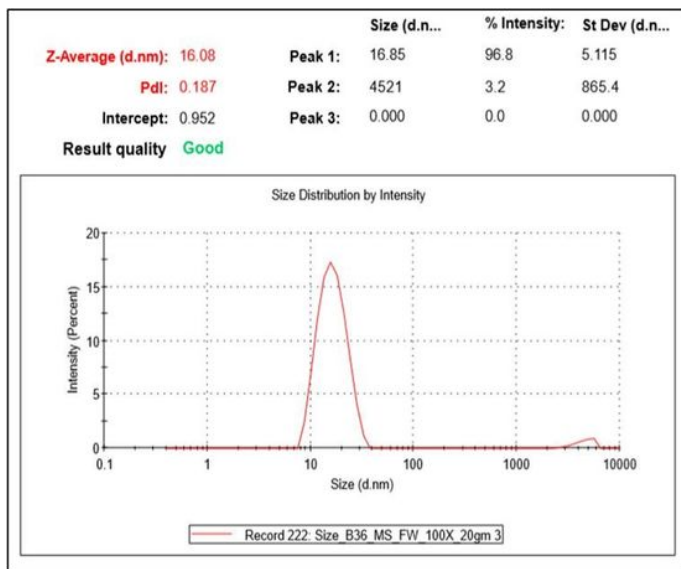


Figure 1

### Pseudoternary phase diagrams





**Fig no. a**

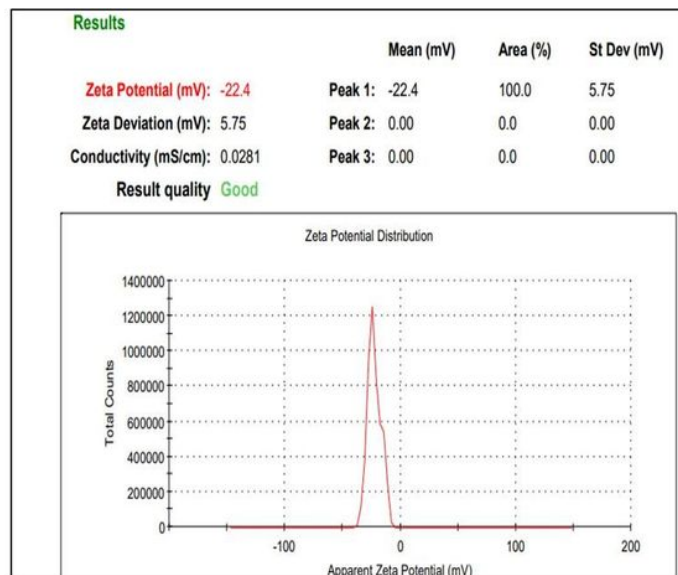


**Fig no. b**

**Figure 2**

Particle size analysis and zeta potential graph of optimized batch

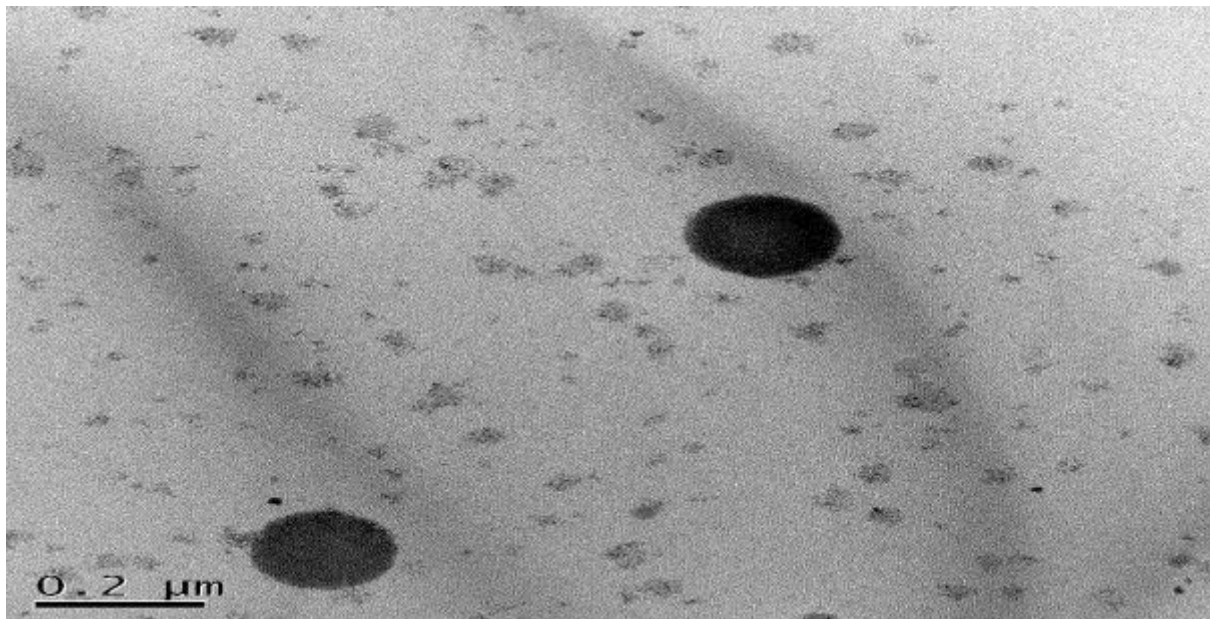


**Figure 3**

TEM image of nanoemulsion at 200nm scale.

**In-vitro drug diffusion from nanoemugel**

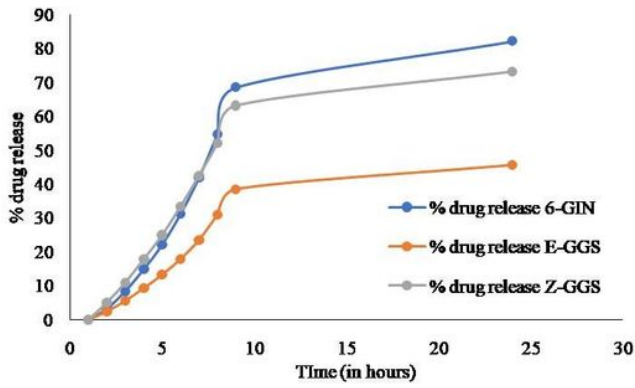


**Fig no. a**

**Ex-vivo drug diffusion from nanoemugel**

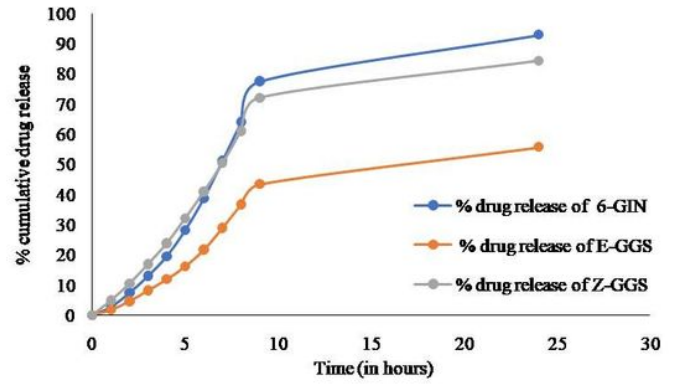


**Fig no. b**

**Figure 4**

**a) In vitro drug release and b) ex vivo drug release from nanoemugel**

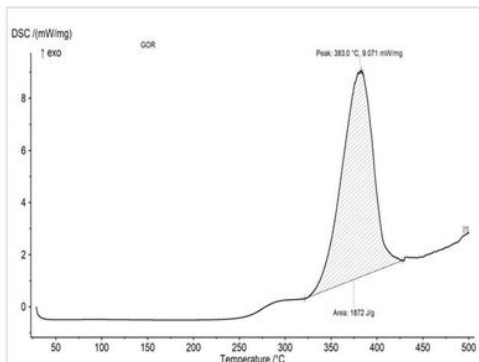


**Fig no. a**

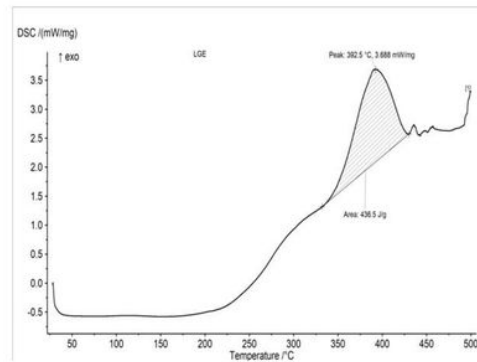


**Fig no. b**

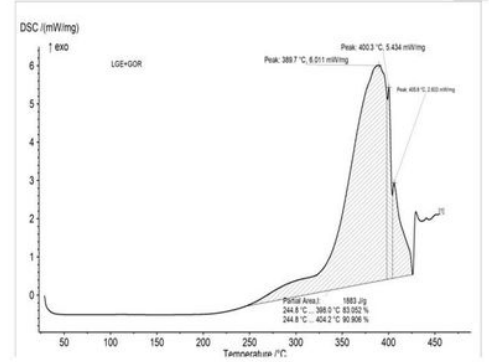


**Fig no. c**

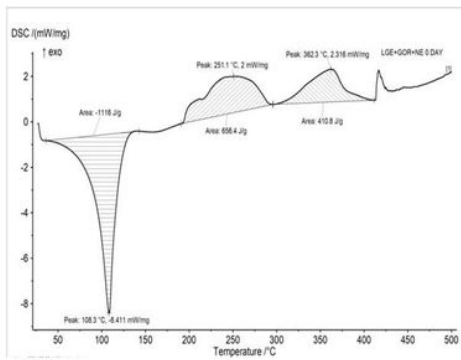


**Fig no. d**

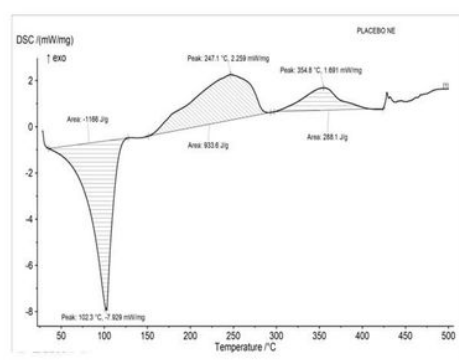


**Fig no. e**

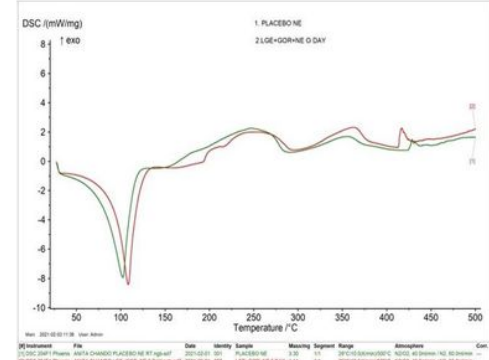


**Fig no. f**

**Figure 5**

**DSC images a) Gingerol b) Lipid guggul extract c) Mixture of gingerol and lipid guggul extract d) placebo e) drug loaded NGE f) overlay of Placebo and drug loaded NGE.**

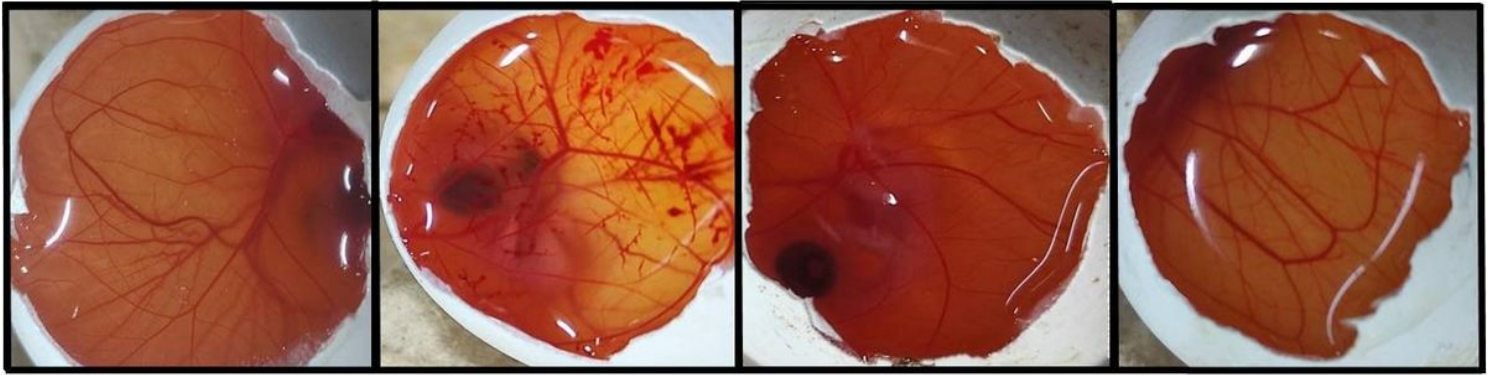


**Fig no. a**

**Fig no. b**

**Fig no. c**

**Fig no. d**

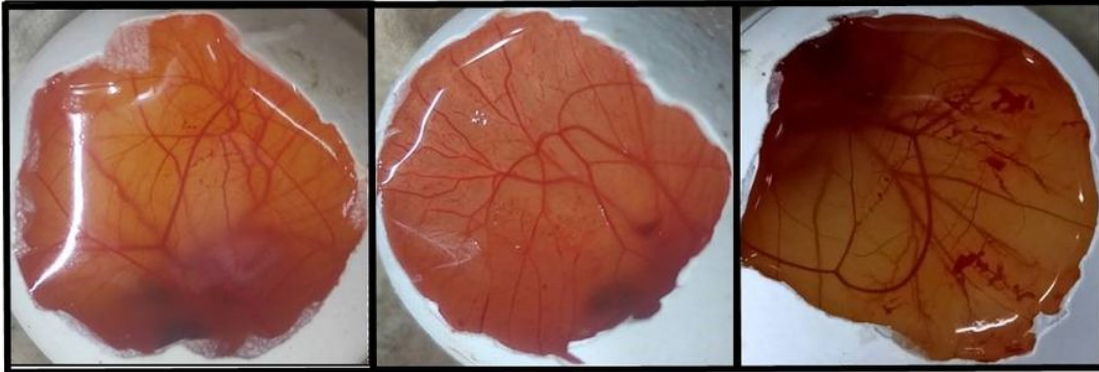


**Fig no. e**

**Fig no. f**

**Fig no. g**

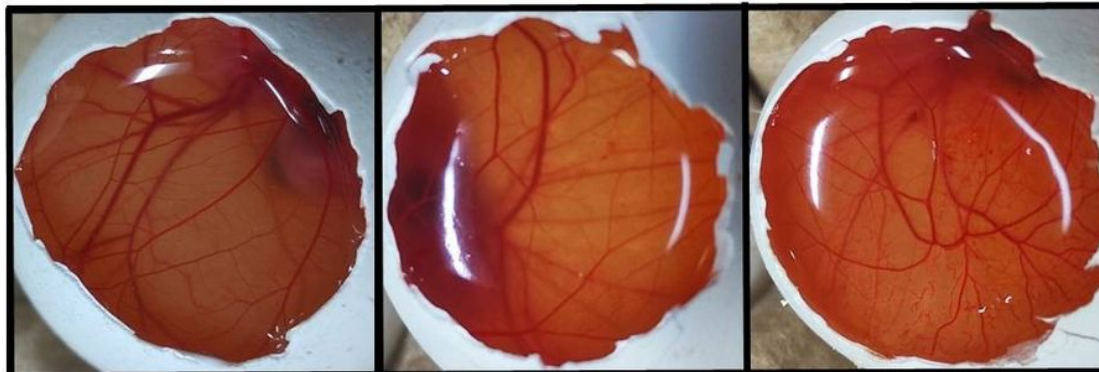


**Fig no. h**

**Fig no. i**

**Fig no. j**

**Figure 6**

HET CAM images a) Negative control (0.9% NaCl) b) Positive control (0.1N NaOH) c) Vehicle (Olive oil) d) 0.75% Carbopol Ultrez 10 NF e) 1% LGE solution f) 1% GOR solution g) 1%LGE+1% GOR solution h) Placebo NEG i) 1% LGE+1% GOR NEG j) Diclofenac sodium Emulgel

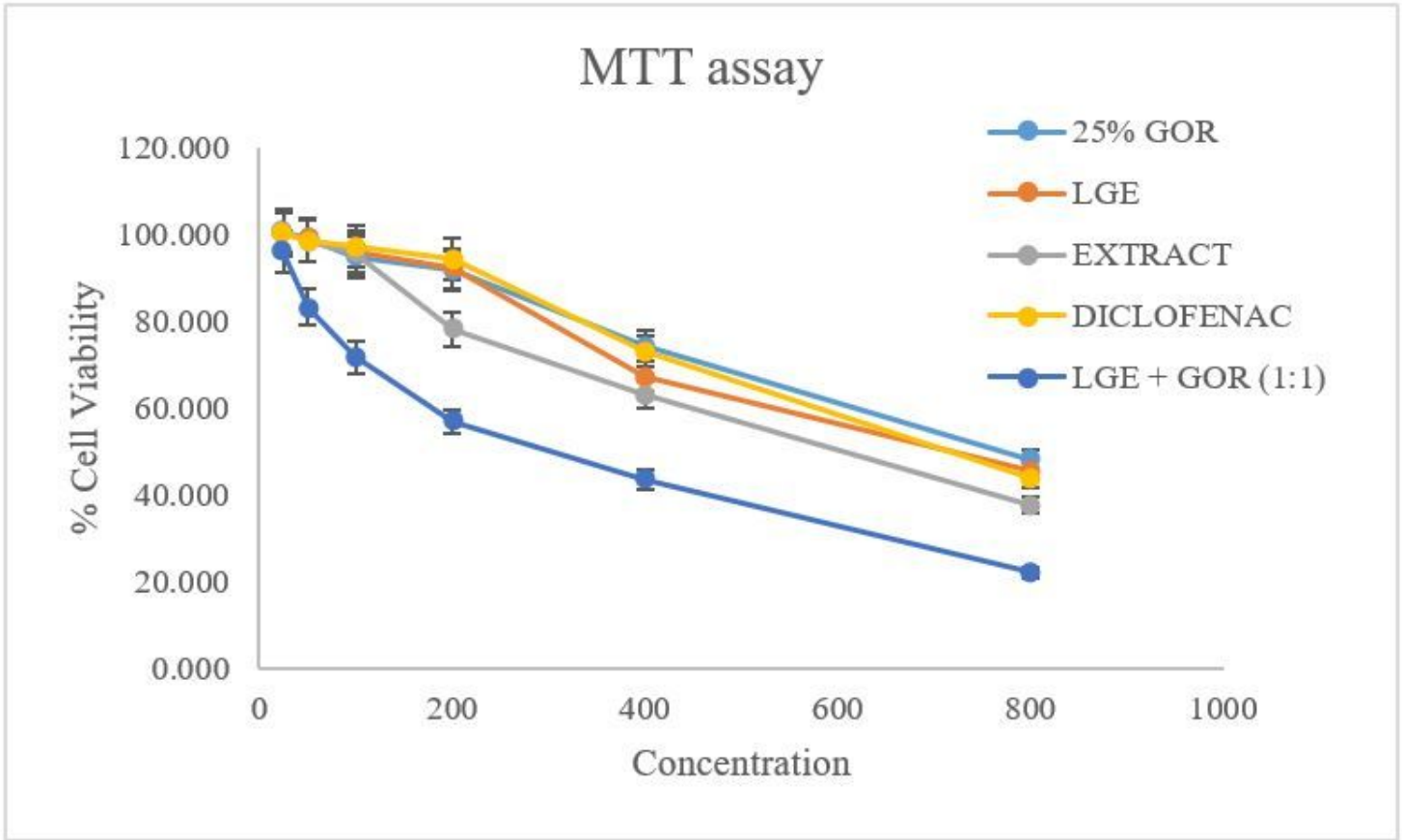


Figure 7

MTT assay of 25% GOR, LGE, extract, Diclofenac, LGE+GOR (1:1)

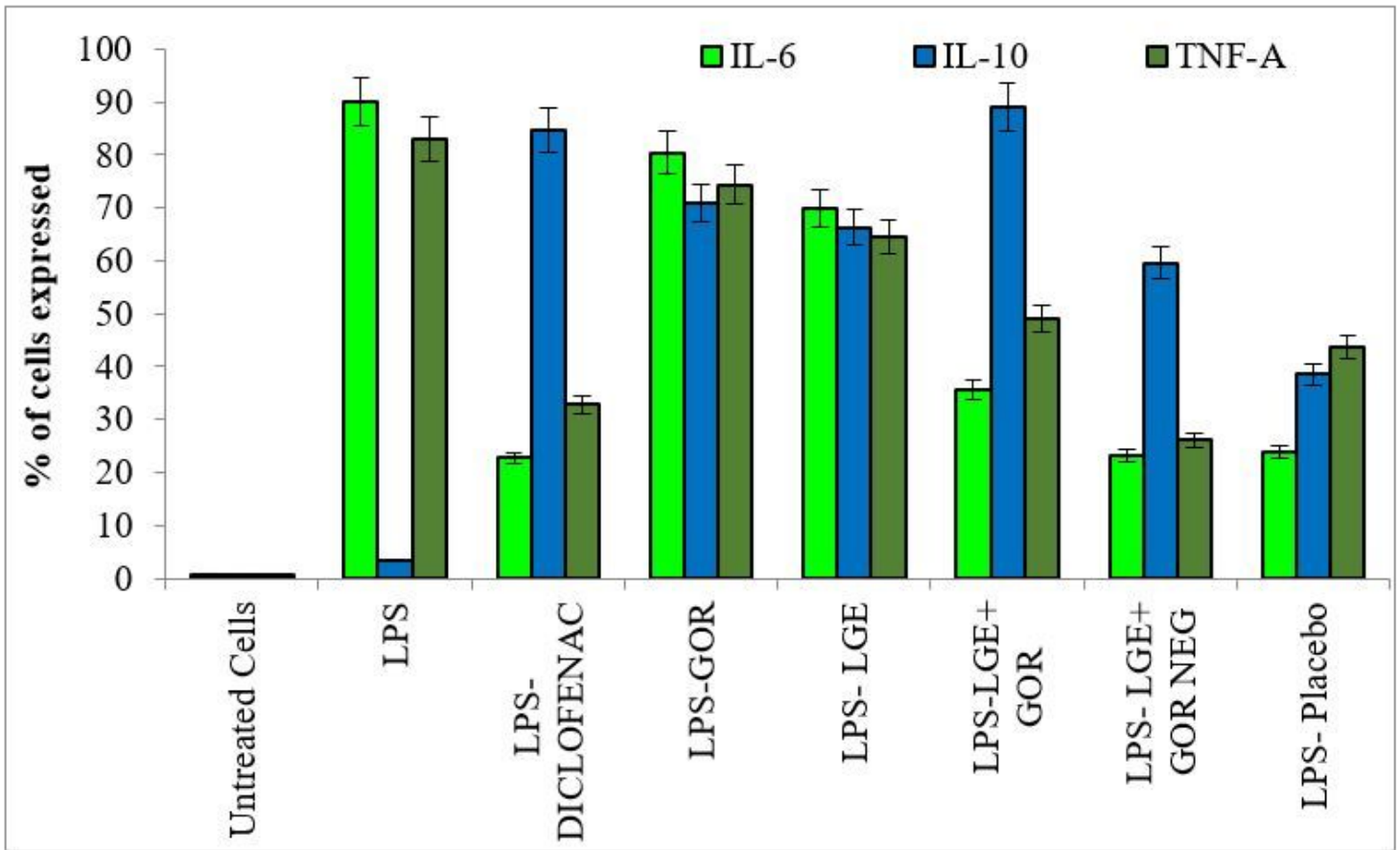


Figure 8

Cytokine expression of IL-6, IL-10 & TNF-α in LPS induced cells.

### Paw edema

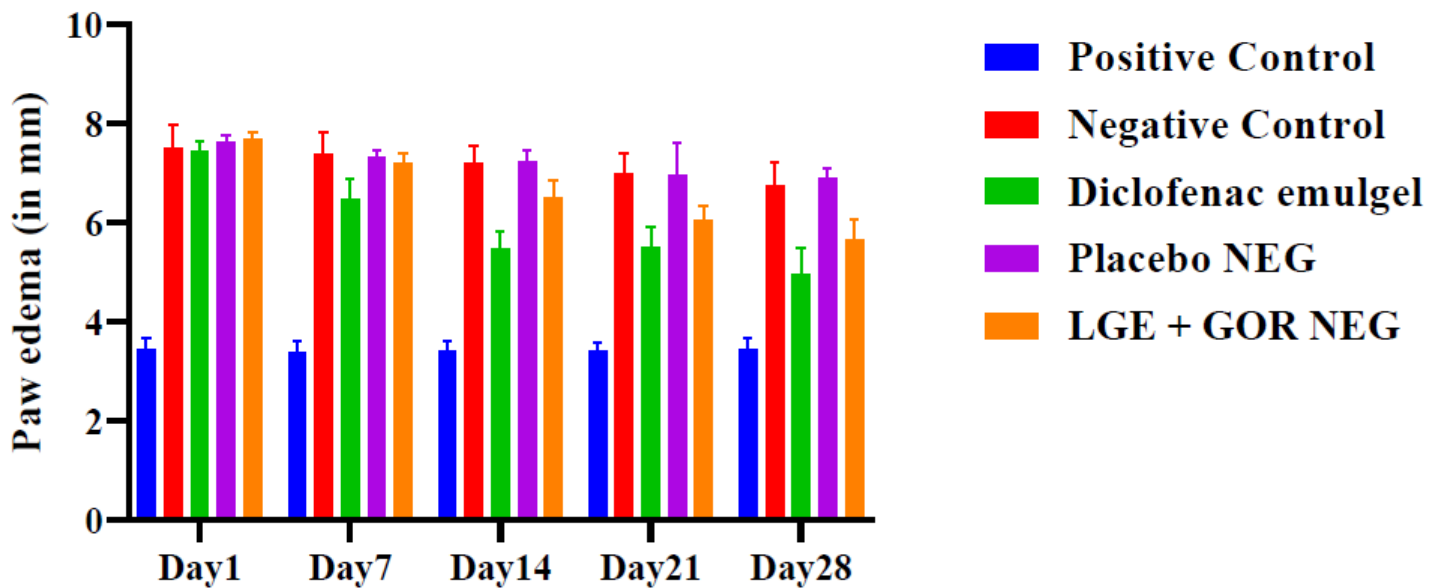


Figure 9

Paw edema measurement of CFA induced rats treated with diclofenac emugel, Placebo NEG and LGE+GOR NEG

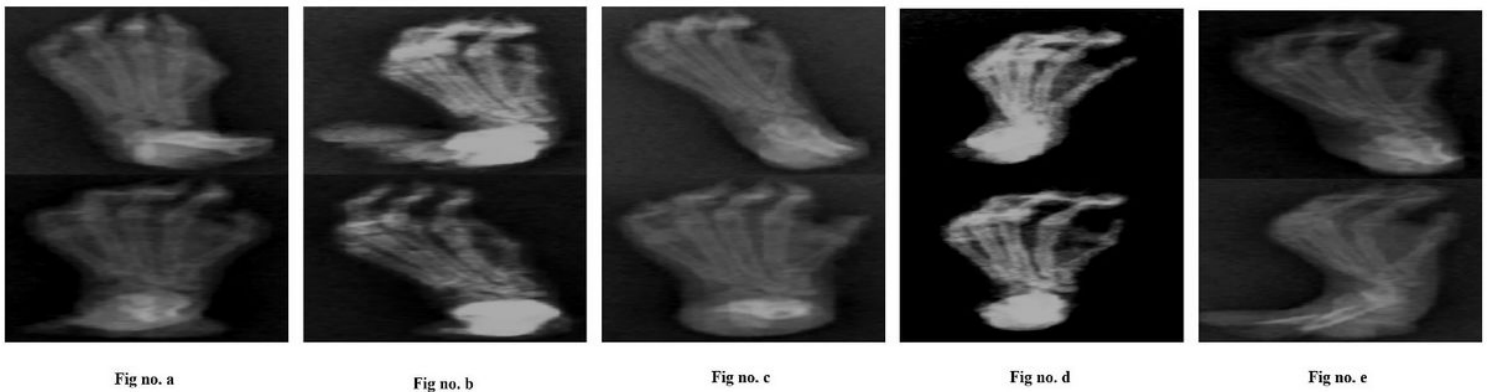


Figure 10

X-ray of left hind paw of CFA induced rats a) Positive control b) Negative control c) Diclofenac nanoemugel d) Placebo NEG e) LGE + GOR NEG

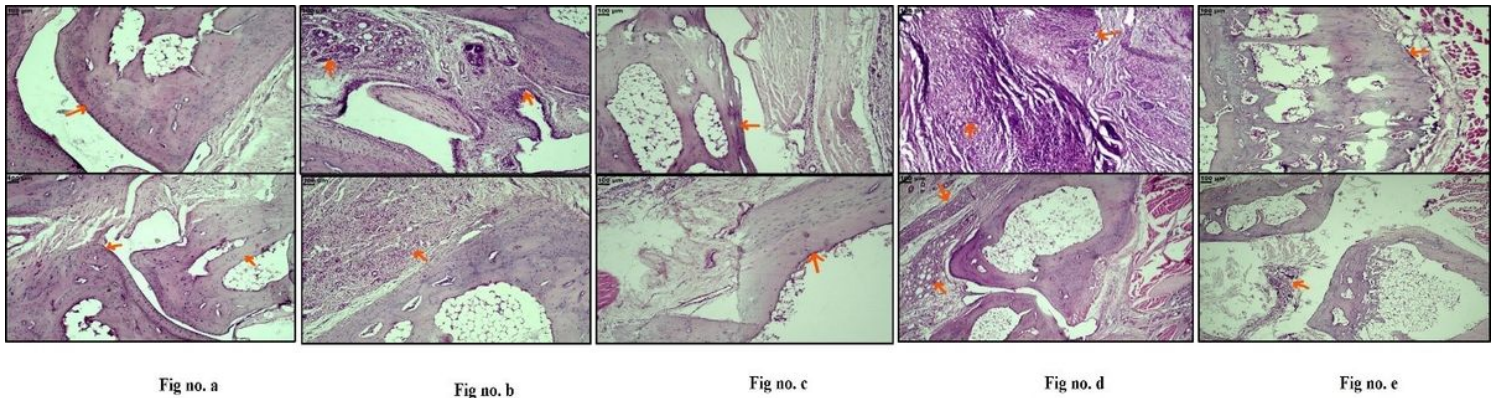


Figure 11

Histopathological evaluation of left hind paw of CFA induced rats a) Positive control b) Negative control c) Diclofenac nanoemugel d) Placebo NEG e) LGE + GOR NEG

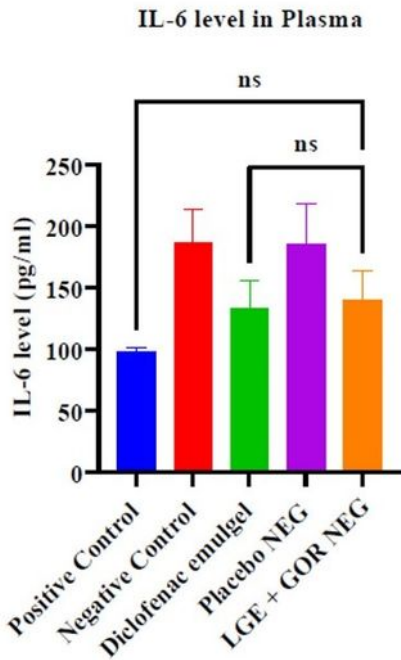


Fig no. a

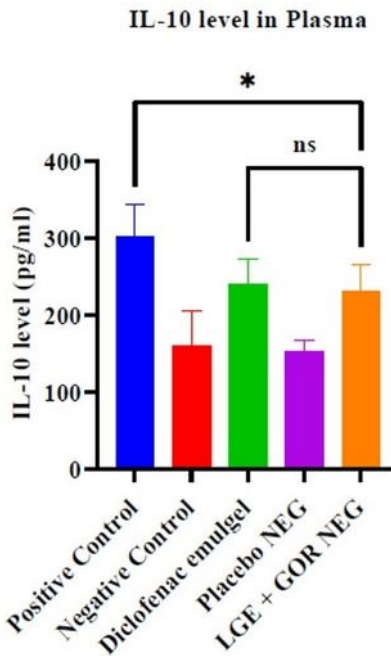


Fig no. b

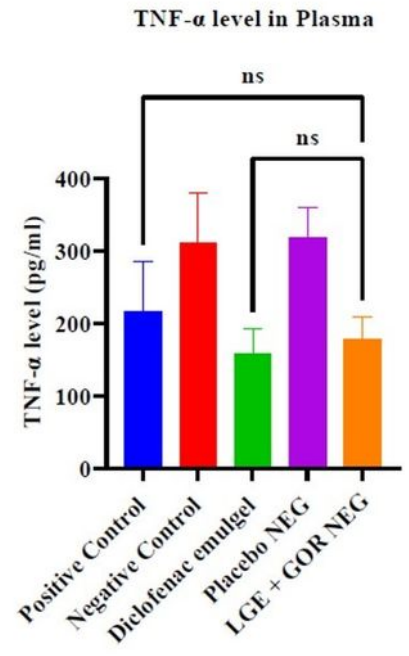


Fig no. c

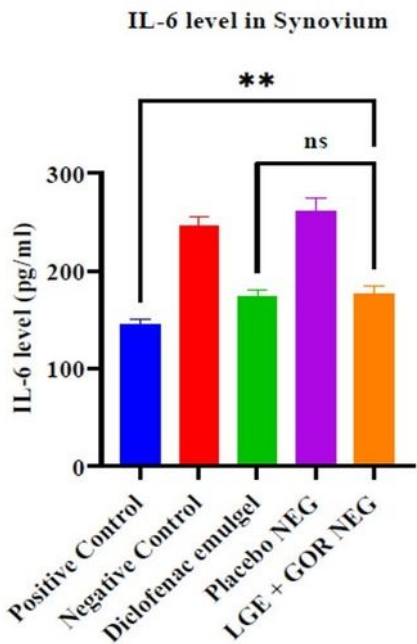


Fig no. d

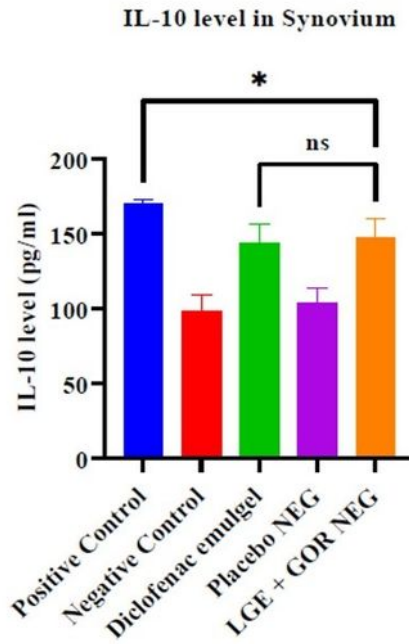


Fig no. e

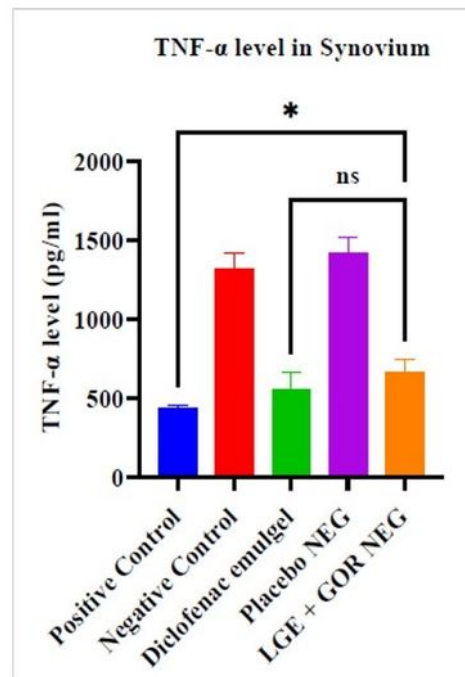


Fig no. f

Figure 12

Cytokines levels in plasma and synovium of CFA induced rats observed after 28days of treatment a) IL-6 in Plasma b)IL-10 in Plasma c) TNF-α in Plasma, d) IL-6 in synovium, e) IL-10 in synovium and f) TNF-α in Plasma.

Note: ns- non significant ( $p > 0.05$ ), \* - significant ( $p \leq 0.05$ ), \*\*very significant ( $p \leq 0.01$ )

## Supplementary Files

This is a list of supplementary files associated with this preprint. Click to download.

- [GraphicalAbstract.jpg](#)